JAERI-Research
95-065

STABILITY OF TOROIDAL ALFVÉN EIGENMODE IN JT-60 SUPER UPGRADE

October 1995

Takahisa OZEKI, Chio Z. CHENG* and Keisuke NAGASHIMA

日本原子力研究所
Japan Atomic Energy Research Institute

本レポートは，日本原子力研究所が不定期に公刊している研究報告書です。
入手の問合わせは，日本原子力研究所技術情報部情報資料課（〒319-11 茨城県那珂郡東海村）あて，お申し越しください。なお，このほかに財団法人原子力弘済会資料センター（〒319-11 茨城県那珂郡東海村日本原子力研究所内）で複写による実費頒布をおこなっております。

This report is issued irregularly.
Inquiries about availability of the reports should be addressed to Information Division, Department of Technical Information, Japan Atomic Energy Research Institute, Tokai-mura, Naka-gun, Ibaraki-ken 319-11, Japan.

© Japan Atomic Energy Research Institute, 1995

編集兼発行　日本原子力研究所
印　　刷　㈱原子力資料サービス

JAERI－Research 95－065

Stability of Toroidal Alfvén Eigenmode in JT-60 Super Upgrade

Takahisa OZEKI, Chio Z. CHENG* and Keisuke NAGASHIMA

Department of Fusion Plasma Research
Naka Fusion Research Establishment
Japan Atomic Energy Research Institute
Naka-machi, Naka-gun, Ibaraki-ken

(Received September 11, 1995)

The theoretical predictions of Toroidal Alfvén Eigenmode (TAE) stability are obtained for typical plasmas with different plasma current in the JT-60 Super Upgrade (JT-60SU). TAE modes are predicted by using the NOVA-K code for self-consistent MHD equilibrium obtained by the ACCOME code. In the high current plasma (10MA), because the pressure gradient of the hot particle, ∇P_h, is small due to high density and V_h/V_A is less than unity due to high toroidal field (6.25Tesla), the TAE mode is stable for the low toroidal mode number n to the medium n ($\leq$15). Here, V_h/V_A is the ratio of the hot particle velocity to the Alfvén velocity. On the other hand, in the low current plasma (3 MA) with the 3Tesla toroidal field, the value of V_h/V_A increases above 1.0 due to the increase of the density, and the TAE mode becomes unstable due to the large pressure gradient ∇P_h and large beta of the hot particle, $\langle \beta_h \rangle$. Further increase of the density and the temperature makes the bootstrap current large so that the NB power required for the current drive decreases. Consequently, both of ∇P_h and $\langle \beta_h \rangle$ decrease, and the TAE modes are stabilized by the ion Landau damping.

Keywords: TAE Mode Stability, Steady-state, N-NBI, α-particle, JT-60SU, NOVA-K

* Princeton Plasma Physics Laboratory

ＪＴ－６０ Super Upgarde のトロイダル・アルフベン固有モード安定性

日本原子力研究所那珂研究所炉心プラズマ研究部
小関　隆久・Chio Z. CHENG*・永島　圭介

（1995年９月11日受理）

ＪＴ－６０ Super Upgarde（ＪＴ－６０ＳＵ）における異なる電流を持つ代表的なプラズマに対して，理論的に予想されるトロイダル・アルフベン固有モード（ＴＡＥモード）安定性を求めた。ＡＣＣＯＭＥコードによって求められた自己矛盾のない平衡に対し，ＮＯＶＡ－Ｋコードを用いてＴＡＥモード安定性を解析した。高電流プラズマ（１０ＭＡ）の場合，高エネルギ粒子の圧力勾配∇P_hは高密度のため減少し，V_h/V_Aは高磁場（６．２５Ｔ）のため１より小さくなる。このため，ＴＡＥモードは低トロイダル番号ｎと中間ｎ（≤１５）において安定となる。ここで，V_h/V_Aは高エネルギ粒子の速度とアルフベン速度の比である。一方，低電流プラズマ（３ＭＡ／３Ｔ）の場合，プラズマ密度の上昇により$V_h/V_A>1$になり，高い圧力勾配∇P_hと大きな$\langle\beta_h\rangle$のためにＴＡＥモードは不安定となる。さらに，密度及び温度が上昇すると，ブートストラップ電流は増加し，電流駆動に必要なＮＢパワーは減少する。この結果，∇P_hと$\langle\beta_h\rangle$の両方が減少しＴＡＥモードはイオンのランダウ減衰により安定化される。

那珂研究所：〒311-01　茨城県那珂郡那珂町向山801-1
＊ プリンストン大学プラズマ物理研究所

Contents

目　　次

1. INTRODUCTION

A global Alfvén wave called the toroidal Alfvén eigenmode (TAE mode) was theoretically discovered by Cheng[1,2]. In a toroidal configuration, because of the non-uniformity of the toroidal magnetic field, coupling of different poloidal harmonics breaks up the shear Alfvén continuous spectrum and creates discrete shear Alfvén eigenmodes inside the continuum gap. The poloidal harmonic coupling is located around $q(r) = (m_1 + m_2)/2n$ surfaces with corresponding local shear Alfvén frequencies $\omega_0 = [(m_1 - m_2)V_A(r)/2q(r)R]$, where m_1 and m_2 are two different poloidal mode numbers, n is the toroidal mode number, R is the major radius, and $V_A(r)$ and $q(r)$ are the Alfvén velocity ($= B/(n_i M_i)^{1/2}$: n_i is the ion density and M_i the ion mass) and the safety factor at the minor radius, r. The global solution with a discrete eigenvalue due to the coupling of $m_1(= m)$ and $m_2(= m + 1)$ poloidal harmonics is the TAE mode. The TAE mode can be destabilized by a large, centrally peaked population of fast ions with velocities near the Alfvén speed[2-5] such as fusion alpha particles or energetic NBI ions. The TAE mode has been experimentally observed in TFTR [6], DIII-D [7], JT-60U [8] and other NBI or ICRF-powered tokamaks, and is found to be capable of causing significant loss of fast ions.

In the future tokamak such as JT-60 Super Upgrade (JT-60SU)[9], the TAE mode may become unstable due to high energy particles. JT-60SU is being designed to investigate physics of steady-state tokamak plasmas based on D-D operation. The mission of JT-60SU is to establish the integrated basis of physics and technology for a steady state tokamak reactor. The main issue of physics is the simultaneous achievement and sustainment of high-β_p, high-β_N, non-inductive current drive, high confinement, and divertor heat and particle control. Here, $\beta_p = 2\langle p\rangle/\langle B_p\rangle^2$ and $\beta_N = \beta_t/(I_p/aB_t)$, where $\beta_t = 2\langle p\rangle/\langle B_t\rangle^2$, I_p is the plasma current, a is the minor radius, and B_t is the toroidal field. The basic design parameters of JT-60SU are shown in Table 1. To produce a steady-state plasma, a tangentially injecting NBI system is employed for non-inductive current drive in addition to as a plasma heating source. The NBI system employed in JT-60SU is the negative-ion based neutral beam injection (N-NBI) with a beam energy of 500keV. The purpose of this paper is to predict the TAE mode stability due to such high energy particles.

In JT-60SU, for the 500keV N-NBI, the beam velocity, V_h, is $6.92 \times 10^6 m/s$ and is close to the typical Alfvén speed, $V_A \sim 5 \times 10^6 m/s$, in a toroidal field of 3 Tesla. If $V_h \geq V_A$, the circulating energetic particles can destabilize shear Alfvén waves via inverse Landau damp-

ing through the $\omega = k_{\|}v_{\|}$ wave-particle resonance. Here, $k_{\|} = (m - nq)/qR$ is the parallel wavenumber for linealized waves that are Fourier decomposed as $\exp[i(m\theta - n\zeta - \omega t)]$. To overcome the velocity space Landau damping by the inverse Landau damping associated with ω_{*h}, it requires roughly that $\omega_{*h} \geq \omega_A = V_A/qR$. If this condition is satisfied, the damping associated with the velocity gradient at the resonance velocity becomes smaller than the instability drive associated with the radial gradient of the fast ion distribution. Here, ω_{*h} ($= (m/r)(T_h/e_hB)(1/n_h)(dn_h/dr)$) is the diamagnetic drift frequency. If the beam energy is large or the spatial gradient of hot particle pressure becomes large, the unstable condition is easily satisfied. Therefore, in JT-60SU there is a possibility that the TAE mode can be unstable routinely. The loss of high energy particles due to the TAE mode may restrict the steady-state plasma operations with high confinement.

In Section 2, we describe the computational techniques used in obtaining equilibrium data as well as for analyzing the ideal TAE mode stability. In Section 3, results of the TAE mode stability analysis for three typical plasmas with 10MA, 6MA and 3MA are obtained. The effect of α particles also discussed. Finally, results are summarized in Section 4.

2. CALCULATION PROCEDURE

2.1 EQUILIBRIUM

To analyze a steady state plasma, it is important to generate self-consistent equilibria because the current profile and the pressure profile are strongly coupled in a high β_p plasma. The equilibria used in this paper are generated by utilizing the free boundary MHD equilibrium code including non-inductive plasma current, ACCOME[10]. In the ACCOME code, the geometric parameters and the profile data ($T_i(r)$, $T_e(r)$, $n_e(r)$ and $Z_{eff}(r)$) are required for the input data. Here, r/a is a normalized effective minor radius ($= \sqrt{V(\psi)/V_{tot}}$). MHD equilibrium is obtained by an iterative calculation with specified values of the total plasma pressure gradient, p' ($= dp/d\psi$), which includes the $\alpha-$particle pressure and the beam pressure, and the current density $< \mathbf{J}\cdot\mathbf{B} >$ of the ohmic current, the bootstrap current and the beam driven current. The bootstrap current for multi-species ions including fast ions is numerically evaluated by using the Hirshman-Sigmar's moment approach in the neo-classical theory. The beam driven current is evaluated by analytical eigen functions of the Fokker-Planck equation.

For the inductive plasma such as a high current plasma with 10MA, MHD equilibrium is solved with a restriction that the total plasma current is kept constant by the regulation of one-turn voltage at every iteration step with a constant NBI power. For non-inductive plasmas, the one-turn voltage is kept zero and the NBI power is regulated for a given total current. The following profile functions:

$$n = n_0\{0.8 \times (1-(r/a)^2)^{0.5} + 0.2\}, \quad (1)$$

$$T = T_0\{0.98 \times (1-(r/a)^2) + 0.02\}, \quad (2)$$

are assumed in the present work. The subscript 0 denotes the value at the magnetic axis. n_0 and T_0 ($= T_{i0} = T_{e0}$) are obtained by using the ITER power law[11] with a H-factor of 2 or 3. $Z_{eff}(r)$ is assumed uniform against the minor radius, and the impurity species is assumed to be Carbon. Our procedure is to generate equilibria for typical operational parameters on the JT-60SU configuration. The equilibrium is reconstructed in the NOVA-K code, where the outer flux surface on the (R, Z) plane is re-defined by $R = R_p + a\cos[\theta + \delta\sin\theta]$, $Z = \kappa a \sin\theta$. The fixed parameters are the ellipticity κ, the triangularity δ, the major radius R_p and the minor radius a. For the pressure profile and the q-profile, the following function is used: $P(\tilde{\psi}) = P_0(1-\tilde{\psi}^\lambda)^\mu$, $q(\tilde{\psi}) = q_0 + \tilde{\psi}\{q_s - q_0 + [q_s' - q_s + q_0][(1-\tilde{\psi}_s)(\tilde{\psi}-1)/(\tilde{\psi}-\tilde{\psi}_s)]\}$,

where $\tilde{\psi}_s = [q'_s - q_s + q_0]/\{q'_0 + q'_s - 2[q_s - q_0]\}$, $\tilde{\psi} = (\psi - \psi_0)/(\psi_s - \psi_0)$, ψ_s is evaluated at the plasma edge, and ψ_0 is evaluated at the magnetic axis. The parameters are adjusted to reproduce the pressure profile and the q-profile obtained by the ACCOME code. Figure 1 shows the equilibrium configuration obtained by the ACCOME code and the re-constructed equilibrium used in the NOVA-K code. Both shapes of flux surfaces agree well except near the separatrix. Since the dominant mode of TAE is internal, the influence of the difference of the shape near the separatrix is small.

2.2 TAE STABILITY

The stability of the TAE mode is investigated with a nonvariational kinetic-MHD stability code, NOVA-K[12]. The NOVA-K code, which is the kinetic extension of a previously developed ideal MHD NOVA code[13], employs Fourier expansion in the poloidal angle θ direction and cubic B-spline finite elements in the radial ψ direction for a flux coordinate system (ψ, θ, ζ) with an arbitrary Jacobian. The NOVA-K code evaluates the growth rate of the TAE mode due to the kinetic effects using a perturbative analysis. Here, a conductive wall on the plasma boundary is employed. In addition to the driving terms, the NOVA-K code includes the damping terms, such as electron Landau damping, thermal ion Landau damping and the electron collisional damping.

For high energy particles it is more reasonable to assume a slowing down distribution in energy and a Gaussian in pitch angle. The model used in the following calculation is as follows:

$$F_h(\epsilon, \Lambda, \psi) = A(\psi) \exp\left[-\left(\frac{\Lambda - \Lambda_0}{\Delta}\right)^2\right] / (\epsilon_c^{3/2} + \epsilon^{3/2}), \qquad \epsilon \leq \epsilon_b \tag{3}$$

$$= 0, \qquad \epsilon > \epsilon_b \tag{4}$$

Here, ϵ_c is the beam cut off energy of $200keV$. For the NBI plasma, $\epsilon_b = 500keV$, $\Lambda_0 (= v_\perp^2/v^2) = 0.1$, $\Delta = 0.7$. For α-particle $\epsilon_b = 3.5MeV$ and $\Delta = 1000$ for uniform pitch angle distribution.

3. RESULTS OF TAE MODE STABILITY ANALYSIS

3.1 10MA PLASMA

Plasmas with higher plasma current of 10MA are investigated in this section. Since 10MA is the maximum current of JT-60U, the 10MA plasma produced with the high toroidal field of 6.25Tesla is expected to have the maximum plasma performance such as the energy confinement time, the triple product ($n\tau_E T_i$), and the fusion product (Q_{DD}). The long pulse discharge is produced by the ohmic current, the beam-driven current and the bootstrap current. For the volume average density $\langle n_e \rangle$ of $5 \times 10^{19} m^{-3}$ to $8 \times 10^{19} m^{-3}$, the corresponding temperature, T_0, is 16keV to 10keV, using the ITER power law with the H-factor of 2. Figure 2 shows the pressure profile and the current density profile for $\langle n_e \rangle = 5 \times 10^{19} m^{-3}$ ($T_0 = 16keV$ and $n_{e0} = 6.8 \times 10^{19} m^{-3}$). The profile of heat-deposition is not peaked resulting in a parabolic pressure profile of the hot particle.

First, the n=1 TAE mode is investigated. The gap of shear Alfvén continuous spectrum for the n=1 mode as a function of the minor radius is obtained between $(\omega/\omega_A)^2$ =1.1 and 2.1. The discrete global n=1 TAE mode exists inside the continuum gap with the frequency $(\omega/\omega_A)^2$ of 1.89. The eigenfunction ξ_ψ of the n=1 TAE mode has the dominant components of the $m = 1$ and 2 peaking near the q=1.5 surface. Figure 3 shows the stability boundary of the n=1 TAE mode in the $\langle \beta_h \rangle - V_h/V_A$ space for $\langle n_e \rangle$ of $5 \times 10^{19} m^{-3}$ to $8 \times 10^{19} m^{-3}$. Scanning V_h/V_A for obtaining the stability boundary, the plasma density is artificially changed while fixing other equilibrium parameters, though V_A depends on the plasma density so that the equilibrium changes. Above the solid curves, the n=1 TAE mode is unstable. For these equilibria, the value of V_h/V_A (marked ×) is lower than 1.0, and the plasma is stable since the destabilization due to the sideband resonance ($1/3 < V_h/V_A < 1$) is weak. The corresponding profiles of the high energy particle pressure are shown in Fig. 4. As the density increases, the beam deposition shifts from the plasma center to the half radius, resulting in broader pressure profile of high energy particles. However, the q-profile does not change very much because the bootstrap current fraction is less than 20%. The q-profile is kept monotonic and q_0 is around 1.0. Thus, the TAE eigenfunction of these plasmas does not change so that it has similar dominant modes of m=1 and 2, and the unstable region shrinks. Here, we note that the standard operation of 10MA plasma will be performed in the higher density region around $\langle n_e \rangle = 1 \times 10^{20} m^{-3}$ so that the hot particle pressure profile becomes broader than those on Fig. 4.

The growth rate of TAE mode generally increases with the toroidal mode number, n, because

$$\frac{\gamma}{|\omega|} \propto \left(\frac{\partial F_h}{\partial \epsilon} - \frac{nq}{eB\omega} \frac{\partial F_h}{\partial r} \right) \tag{5}$$

Therefore, it is necessary to investigate the stability of higher n modes. Here, we consider the toroidal number, n of 1 to 15 for the plasma with a plasma density of $\langle n_e \rangle = 5 \times 10^{19} m^{-3}$, since it has a relatively large pressure gradient. Figures 5 shows the growth rate due to NBI particles, γ_h, and the ion Landau damping rate, γ_i. The value of γ_h increases with the toroidal mode number. The value of γ_h for $n = 15$ is comparable to the value of γ_i. For $n > 15$, the TAE modes are unstable. Fu and Cheng have studied the finite orbit effect on the high n TAE mode stability [14]. In the case of $k_\theta \rho_\alpha \sim 1$, the growth rate is saturated for both passing particles and trapped particles. Here, k_θ is nq/r and ρ_α is the Larmor radius of the high energy particles. In the 10MA Deuterium plasma, ρ_α is approximately $1.7 \times 10^{-2} m$ so that $k_\theta \rho_\alpha \sim 1$ when $n \sim 20$. Therefore, the TAE growth rate can be expected to saturate or decrease for $n \geq 20$ owing to the finite orbit width effect. Here, the electron Landau damping and the electron collisional damping are negligibly smaller than the thermal ion Landau damping.

3.2 6MA PLASMA

Next, we investigate a discharge of 6MA with a the toroidal field of 5.77 Tesla including α-particles. The TAE stability calculation for the non-inductive plasma including α particles is useful for the prediction of future reactor performance. The energy confinement is assumed to follow ITER power law with the H-factor of 3.0 in this calculation. Figure 6 shows the pressure profile and the current density profile of the non-inductive current drive plasma with $\langle n_e \rangle = 8 \times 10^{19} m^{-3}$ ($T_0 = 16 keV$ and $n_{e0} = 1.1 \times 10^{20} m^{-3}$) produced by the NBI power of 62MW. The bootstrap current fraction increases up to 50% but the q-profile remains monotonic ($q_0 = 1.3$, $q_{95} = 4.6$).

We now discuss the dependence of the averaged density between $\langle n_e \rangle = 6-12 \times 10^{19} m^{-3}$ on TAE stability. Since the H-factor of ITER power law is assumed fixed, the temperature and the required NBI power decrease as the density increases. Results of the stability calculation for the n=3 mode are plotted in Fig. 7. The velocity ratio of V_α / V_A for α

particles is high (> 1.4) enough to destabilize the TAE mode. As the bulk plasma density increases, the temperature decreases and the α particle pressure becomes more peaked (Fig. 8(b)). Thus, the growth rate due to α particles increases with the averaged density, though $\langle \beta_\alpha \rangle$ slightly decreases from 0.15% to 0.10%. The growth rate due to the beam particle becomes positive above $\langle n_e \rangle$ of $7 \times 10^{19} m^{-3}$. The ion Landau damping of Deuterium and Tritium also increases with the density, but since the temperature decreases it can not overcome the growth rate due to the fast ion. In this study, the velocity ratio of V_h/V_A of the beam is around 1.0. $\langle \beta_h \rangle$ is around 0.3-0.2% and the pressure gradient of the beam remains high near the plasma center since the bulk temperature is high.

The growth rate due to the beam ions becomes negative below $\langle n_e \rangle$ of $6 \times 10^{19} m^{-3}$ due to $V_h/V_A < 1.0$. And, the growth rate due to α particles is small in this region. In the low density region ($\langle n_e \rangle < 8 \times 10^{19} m^{-3}$), there is no clear gap across the minor radius, so that the continuum damping can be expected if the TAE mode crosses the continuum near the edge. We conjecture that, in the lower density region ($\langle n_e \rangle < 6 \times 10^{19} m^{-3}$), the TAE modes due to both the beam particles and α particles could be stabilized.

3.3. 3MA PLASMA

Non inductive plasmas with a high beta, which are produced in a low plasma current of 3MA and a low toroidal field of 3 Tesla, is investigated in this section. To obtain a non-inductive plasma, the total current is regulated by the NBI power. A typical MHD equilibrium obtained by ACCOME is given in Fig. 9 which shows the pressure profile and the current density profile for $\langle n_e \rangle = 5.1 \times 10^{19} m^{-3}$. Here, the central temperature $T_0 = 6keV$ and the central density $n_{e0} = 7 \times 10^{19} m^{-3}$ are obtained by assuming the ITER power law with the H-factor of 2, and the plasma profiles of Eq.(1) and (2). A high beta plasma with $\beta_t = 1.9$ and $\beta_p = 1.5$ is obtained. The bootstrap current fraction increases up to 48%, and the full current drive is performed by the NBI power of 38MW. Due to the large bootstrap current, q_0 increases to around 2 ($q_0 = 1.8$, $q_{95} = 5.3$). The locus of heat-deposition is near the plasma center producing a peaked pressure profile of the hot particle. ($P_h \propto (1 - \tilde{\psi}^{0.66})^{1.26}$).

The heat-deposition profile depends on the plasma density, and the beta value of the hot particle $\langle \beta_h \rangle$ is determined from the NBI power and the slowing down time of the NB particles. Here, $\langle \beta_h \rangle = 2\langle p_h \rangle / \langle B^2 \rangle$. The NBI power is regulated to keep the plasma current constant, so that it depends on the bootstrap fraction. Consequently, the hot particle pressure profile and $\langle \beta_h \rangle$ depend on the density and the temperature. Therefore, it is important to obtain the stability boundary on the density and the temperature parameter space and to discuss the characteristics of the TAE mode stability.

Figure 10(a) shows the required NBI power, the bootstrap current fraction and the q-value in the density and temperature space, which are obtained under constant values of the total plasma current and the toroidal field. As the density and the temperature increase, the bootstrap fraction increases due to the increase of β_p. The required NBI power decreases with the increase of the bootstrap current and the temperature due to the improvement of the current drive efficiency. The minimum q-value against the minor radius increases with the density, and the q-profile becomes hollow roughly above the $q_{min} = 2.0$ line (in Fig.10(a)), as shown by cases B and C in Fig. 11(a). The equilibria for each NB power, given by solid circles in Fig 10(a), are generated with the ITER power law with a H-factor of 2.

Figure 10(b) shows the unstable domain for the n=3 TAE mode in the $n_0 - T_0$ space. On the low density region ($n_0 < 4 \times 10^{19} m^{-3}$), $\langle \beta_h \rangle$ is larger than that of the higher

density region and the pressure gradient of the hot particle is high, as shown by curve A in Fig. 11(b). But the TAE mode is stable (open circle in Fig. 10(b)) because the mode is not in resonance with the hot particle due to low V_h/V_A (< 1). As the density increases, the profile of the hot particle becomes broader as shown by curves B and C from the peaked one (Fig. 11(b)), and $\langle\beta_h\rangle$ decreases. The TAE mode, however, becomes unstable above n_{e0} of $5 \times 10^{19} m^{-3}$ because $V_h/V_A > 1$ (solid circle in Fig. 10(b)). But it is stabilized again in the higher temperature region ($T_0 > 8keV$) by the ion Landau damping.

The shear Alfvén continuous spectrum for n=3 as a function of the minor radius is shown in Fig. 12 for each equilibrium A, B and C of Fig.11. The continuous spectrum gap is produced at the crossing point of the poloidal harmonic coupling, and a frequency gap across the minor radius can allow TAE modes to exist without suffering continuum damping. Here, the normalizing Alfvén frequency is defined as $\omega_A = V_A(r_0)/q_s(r_s)R$. On the low density region, the q-profile is monotonically increasing and the q_0 is around 1.0 so that the radial variation of q-value is large (Fig. 11(a)). Because the square of shear Alfvén frequency on the crossing point of continuous spectrum is $[V_A(r)/2q(r)R]^2$, the gap frequency on each minor radius of r is proportional to $1/n_e(r)q^2(r)$. Therefore, a large change of q makes no open gap across the whole minor radius, as shown in Fig. 12(a), for the density profile of Eq. (1). Though the discrete global n=3 TAE mode exists inside the gap, the TAE mode crosses the continuum near the edge, where it experiences continuum damping. Since the magnetic shear near the plasma edge is high, the continuum damping can be strong. However, to obtain the TAE mode based on the ideal MHD theory, it is necessary to avoid the singularity of the eigen function. For the equilibrium corresponding to case A, the TAE mode is obtained by employing a parabolic density profile in stead of the broader profile given by Eq.(1), so that the radial variation of $1/n_e q^2$ becomes small. As the averaged density increases, q_{min} rises and the q-profile becomes more flat as in curves B and C in Fig.11(a), the gap opens against the minor radius (Fig. 12(b)), and the continuum damping can be expected no longer. A typical global TAE mode of n=3 is shown in Fig. 13(a) for case B. Since q_0 is above 2.0, the eigenmode consists of dominant poloidal harmonics with the poloidal mode numbers of 6 to 11, and the dominant harmonic is located near the $q \sim 3$ surface. In the high density region, the bootstrap current is dominant and the q-profile becomes hollow. Since the change of $1/n_e q^2$ is small against the minor radius, a clear gap structure is obtained. For the hollow q-profile (case C), two types of TAE modes are found as shown in Fig. 13(b) and (c), respectively. The first

one ((b)) shows that poloidal harmonics have large radial structure on the both sides of the positive shear region and the negative shear region though the phase is inverse. The second one ((c)) shows that the dominant harmonics of $m = 7 - 9$ overlap each other around the q_{min} region. Note that the second one has 4.5 times larger growth rate than the first one.

If the plasma energy confinement follows the ITER power law with a H-factor of 2, the non-inductive plasma can be obtained at points of solid circles in Fig. 10(a). Comparing Fig. 10(a) with Fig. 10(b), the equilibria for P_{NB} =60MW and 40MW are unstable for the n=3 TAE mode, and the equilibrium for 20MW is stable. If the energy confinement is better than two times of the ITER power law, higher density and higher temperature plasmas can be obtained, and the TAE mode would be stabilized by the ion Landau damping.

4. CONCLUSION

The TAE mode stability of three typical plasmas in JT-60SU is obtained. In the high current plasma (10MA), the pressure profile of the hot particle is broad due to high density and V_h/V_A is less than one due to the high toroidal field (6.25Tesla). Therefore, the TAE mode is stable for low n and medium n (≤ 15). Higher n TAE modes ($n \geq 15$) may be weakly unstable, but further investigations including finite orbit width effects and radiative damping are required. In the 6MA plasma, effects of α particle on the TAE mode stability is investigated. If the confinement time is subject to the ITER power law, then as the density increases, the temperature decreases so that the pressure profile of α particles becomes peaked and $\langle\beta_\alpha\rangle$ slightly decreases. Thus, the growth rate due to α particles increases with the density. In the low current (3MA) and the low field plasma (3 Tesla), the dependence of the bulk density and temperature on the TAE stability is obtained. As the density increases, i.e., V_h/V_A becomes larger than 1.0, the TAE mode becomes unstable. However, the further increase of the density and the temperature makes the bootstrap current large so that the NBI power required for the current drive decreases. The resultant pressure gradient of the hot particle and $\langle\beta_h\rangle$ decreases, and the TAE mode becomes stabilized by the ion Landau damping.

one ((b)) shows that poloidal harmonics have large radial structure on the both sides of the positive shear region and the negative shear region though the phase is inverse. The second one ((c)) shows that the dominant harmonics of $m = 7 - 9$ overlap each other around the q_{min} region. Note that the second one has 4.5 times larger growth rate than the first one.

If the plasma energy confinement follows the ITER power law with a H-factor of 2, the non-inductive plasma can be obtained at points of solid circles in Fig. 10(a). Comparing Fig. 10(a) with Fig. 10(b), the equilibria for P_{NB} =60MW and 40MW are unstable for the n=3 TAE mode, and the equilibrium for 20MW is stable. If the energy confinement is better than two times of the ITER power law, higher density and higher temperature plasmas can be obtained, and the TAE mode would be stabilized by the ion Landau damping.

4. CONCLUSION

The TAE mode stability of three typical plasmas in JT-60SU is obtained. In the high current plasma (10MA), the pressure profile of the hot particle is broad due to high density and V_h/V_A is less than one due to the high toroidal field (6.25Tesla). Therefore, the TAE mode is stable for low n and medium n (≤ 15). Higher n TAE modes ($n \geq 15$) may be weakly unstable, but further investigations including finite orbit width effects and radiative damping are required. In the 6MA plasma, effects of α particle on the TAE mode stability is investigated. If the confinement time is subject to the ITER power law, then as the density increases, the temperature decreases so that the pressure profile of α particles becomes peaked and $\langle\beta_\alpha\rangle$ slightly decreases. Thus, the growth rate due to α particles increases with the density. In the low current (3MA) and the low field plasma (3 Tesla), the dependence of the bulk density and temperature on the TAE stability is obtained. As the density increases, i.e., V_h/V_A becomes larger than 1.0, the TAE mode becomes unstable. However, the further increase of the density and the temperature makes the bootstrap current large so that the NBI power required for the current drive decreases. The resultant pressure gradient of the hot particle and $\langle\beta_h\rangle$ decreases, and the TAE mode becomes stabilized by the ion Landau damping.

Acknowledgements

This work has been done under the US-Japan collaboration program. The author (T.O.) would like to express his gratitude to Dr. G.Y.Fu of PPPL for fruitful discussions. The authors also greatly appreciate Dr. M.Azumi and Dr. M.Kikuchi of JAERI for their continuous support and fruitful discussion.

References

[1] C.Z.CHENG, et al., Ann. Phys. NY 161 (1985) 21.

[2] C.Z.CHENG, et al., Phys. Fluids 29 (1986) 3695.

[3] G.Y.FU, et al., Phys. Fluids B 1 (1989) 1949.

[4] J.W.VAN DAM, et al., Fusion Technol. 18 (1990) 461.

[5] R.BETTI, et al., Phys. Fluids B 4 (1992) 1465.

[6] K.L.WONG, et al., Phys. Rev. Lett. 66 (1991) 1874.

[7] W.W.HEIDBRINK, et al., Nucl. Fusion 31 (1991) 1635.

[8] H.KIMURA, Phys. Lett. A 199 (1995) 86. SAIGUSA, M., et al., Plasma Phys. Control. Fusion 37 (1995) 295.

[9] H.NINOMIYA, et al., in Plasma Physics and Controlled Nuclear Fusion Research 1994 (Proc. 15th Int. Conf. Seville, 1994), IAEA, Vienna (1993) F-1-I-1.

[10] K.TANI, et al., J. of Comput. Phys. 98 (1992) 332.

[11] P.N.YUSHMANOV, et al., Nucl. Fusion 30 (1990) 1999.

[12] C.Z.CHENG, Phys. Rep. 211 (1992) 1.

[13] C.Z.CHENG, et al., J. of Comput. Phys. 71 (1987) 124.

[14] G.Y.FU, et al., Phys. Fluids B 4 (1992) 3722.

Acknowledgements

This work has been done under the US-Japan collaboration program. The author (T.O.) would like to express his gratitude to Dr. G.Y.Fu of PPPL for fruitful discussions. The authors also greatly appreciate Dr. M.Azumi and Dr. M.Kikuchi of JAERI for their continuous support and fruitful discussion.

References

[1] C.Z.CHENG, et al., Ann. Phys. NY 161 (1985) 21.

[2] C.Z.CHENG, et al., Phys. Fluids 29 (1986) 3695.

[3] G.Y.FU, et al., Phys. Fluids B 1 (1989) 1949.

[4] J.W.VAN DAM, et al., Fusion Technol. 18 (1990) 461.

[5] R.BETTI, et al., Phys. Fluids B 4 (1992) 1465.

[6] K.L.WONG, et al., Phys. Rev. Lett. 66 (1991) 1874.

[7] W.W.HEIDBRINK, et al., Nucl. Fusion 31 (1991) 1635.

[8] H.KIMURA, Phys. Lett. A 199 (1995) 86. SAIGUSA, M., et al., Plasma Phys. Control. Fusion 37 (1995) 295.

[9] H.NINOMIYA, et al., in Plasma Physics and Controlled Nuclear Fusion Research 1994 (Proc. 15th Int. Conf. Seville, 1994), IAEA, Vienna (1993) F-1-I-1.

[10] K.TANI, et al., J. of Comput. Phys. 98 (1992) 332.

[11] P.N.YUSHMANOV, et al., Nucl. Fusion 30 (1990) 1999.

[12] C.Z.CHENG, Phys. Rep. 211 (1992) 1.

[13] C.Z.CHENG, et al., J. of Comput. Phys. 71 (1987) 124.

[14] G.Y.FU, et al., Phys. Fluids B 4 (1992) 3722.

Table 1 Main Machine parameters of JT60SU

Parameters		*Values*
Toroidal field at $4.8m$	B_t	$6.25T$
Maximum plasma current	I_p	$10MA$
Major radius	R_p	$4.8m$
Minor radius	a	$1.4m$
Aspect ratio	A	3.43
Elongation	κ	1.8
Triangularity	δ	0.4
Pulse length		$> 2000s$ for full CD

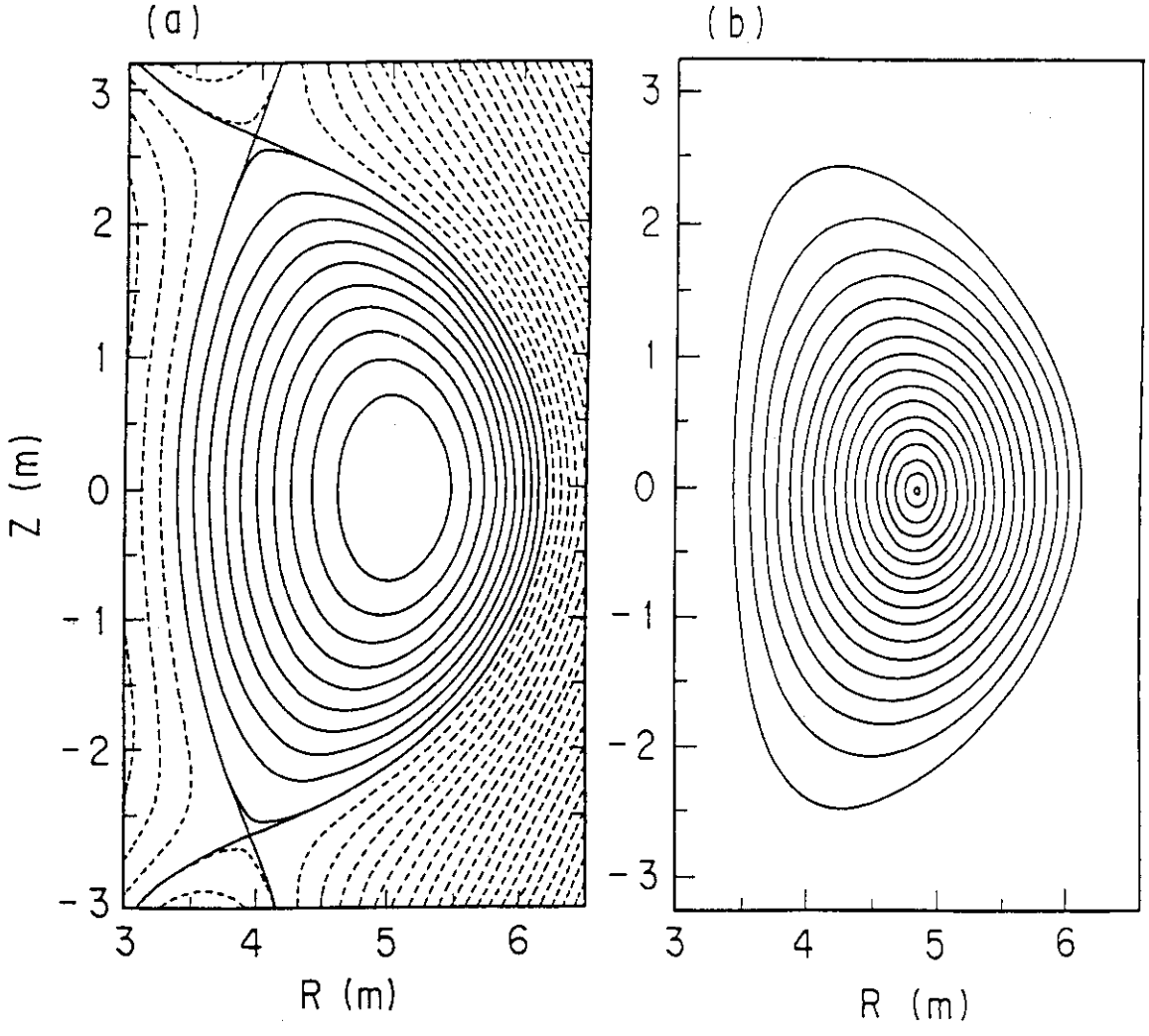

Fig.1 (a) The flux surfaces of the JT-60SU equilibrium by the ACCOME code and (b) the flux surfaces the re-constructed equilibrium for the calculation of NOVA-K code.

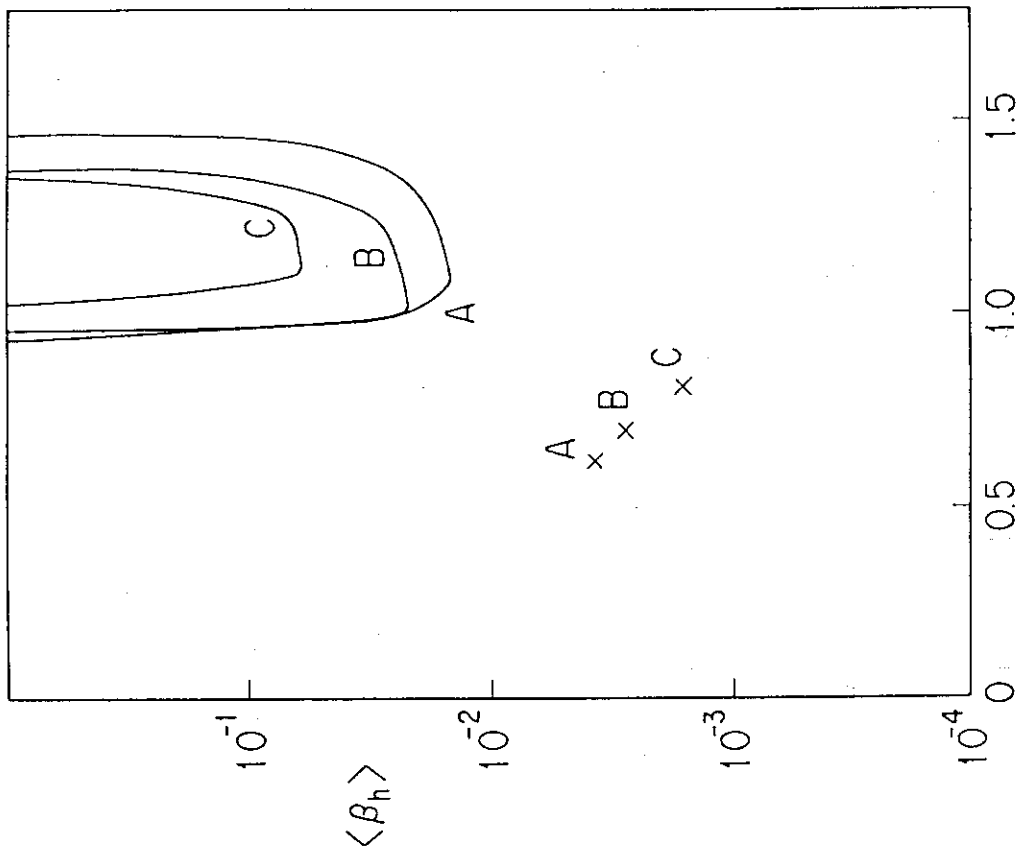

Fig.3 The critical volume averaged $\langle \beta_h \rangle$ versus V_h/V_A stability curve for the equilibrium of A: $\langle n_e \rangle = 5\times10^{19}m^{-3}$, B: $\langle n_e \rangle = 6\times10^{19}m^{-3}$ and C: $\langle n_e \rangle = 8\times10^{19}m^{-3}$ with 10MA plasma current, 6.25T toroidal field, and T_{io} = 12-16keV. The × are points for each equilibrium.

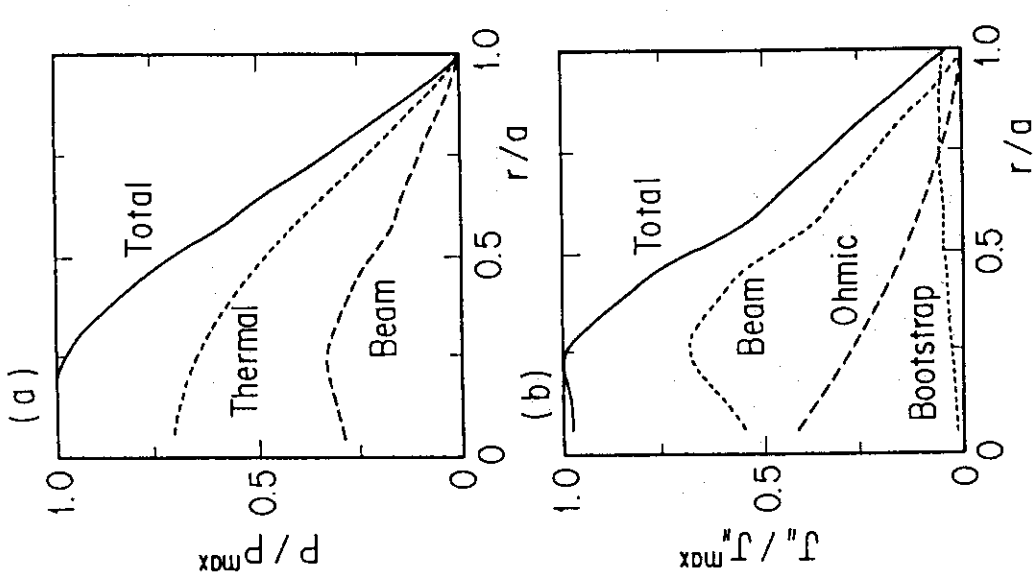

Fig.2 (a) The pressure profile and (b) the current profile of a JT-60SU equilibrium, which has 10MA plasma current, 6.25T toroidal field, $\langle n_e \rangle = 5.0\times10^{19}m^{-3}$ and T_{io} = 16keV.

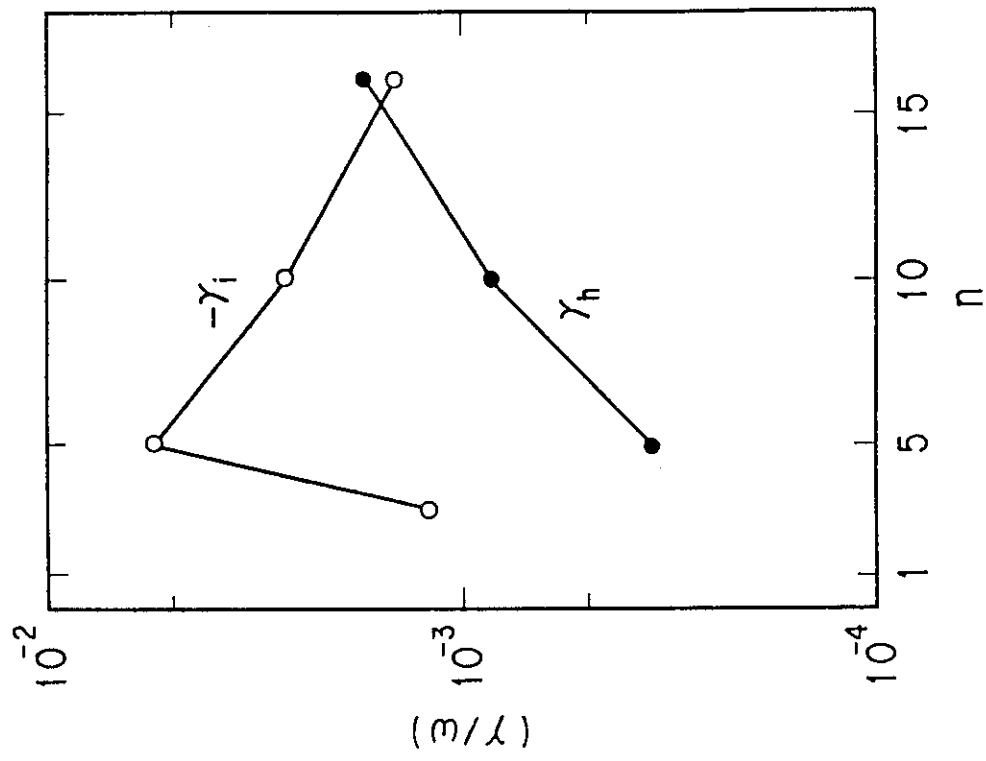

Fig.5 The toroidal number n dependence of the grow rates γ_h due to beam particles and the damping rates γ_i due to ion Landau damping for the equilibrium of A in Fig.3.

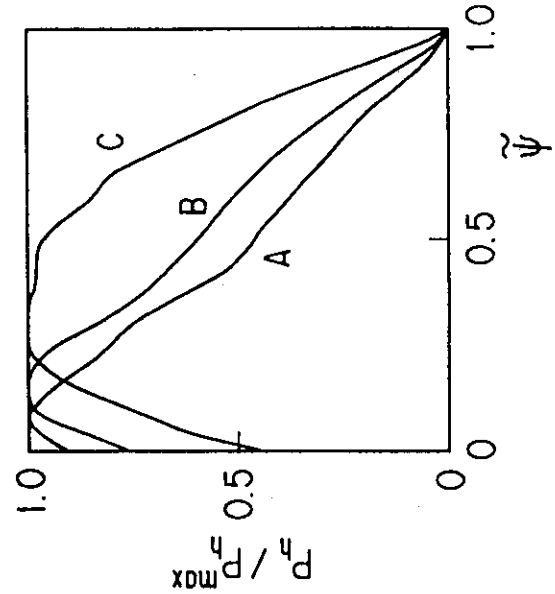

Fig.4 The beam pressure P_h profile.
A-C correspond to those on Fig.3.

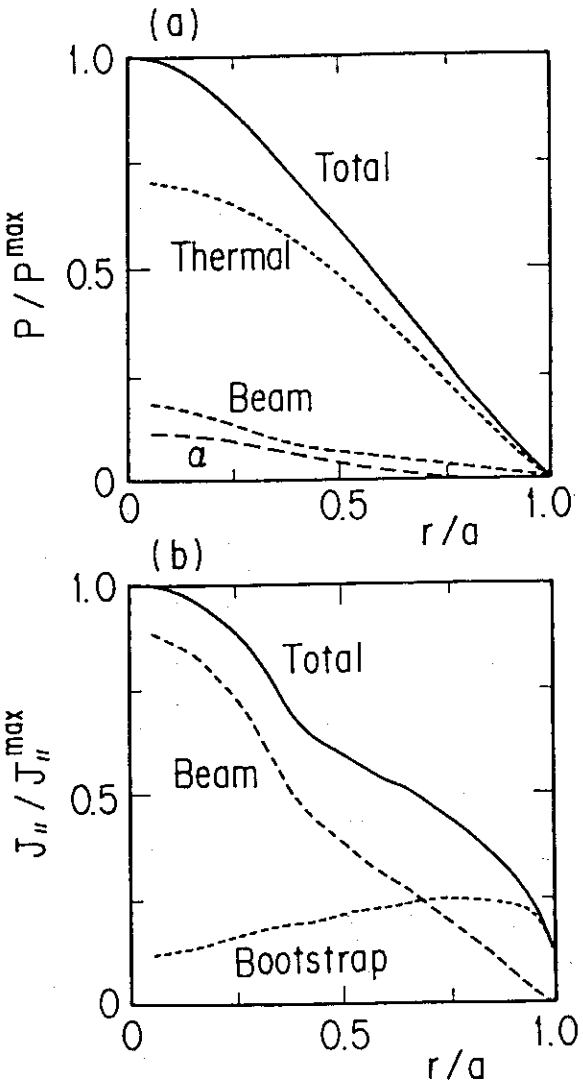

Fig.6 (a) The pressure profile and (b) The current profile of an equilibrium, including α particles, which has 6MA plasma current, 5.77T toroidal field, $\langle n_e \rangle = 8\times10^{19}m^{-3}$ and T_{io} = 16keV.

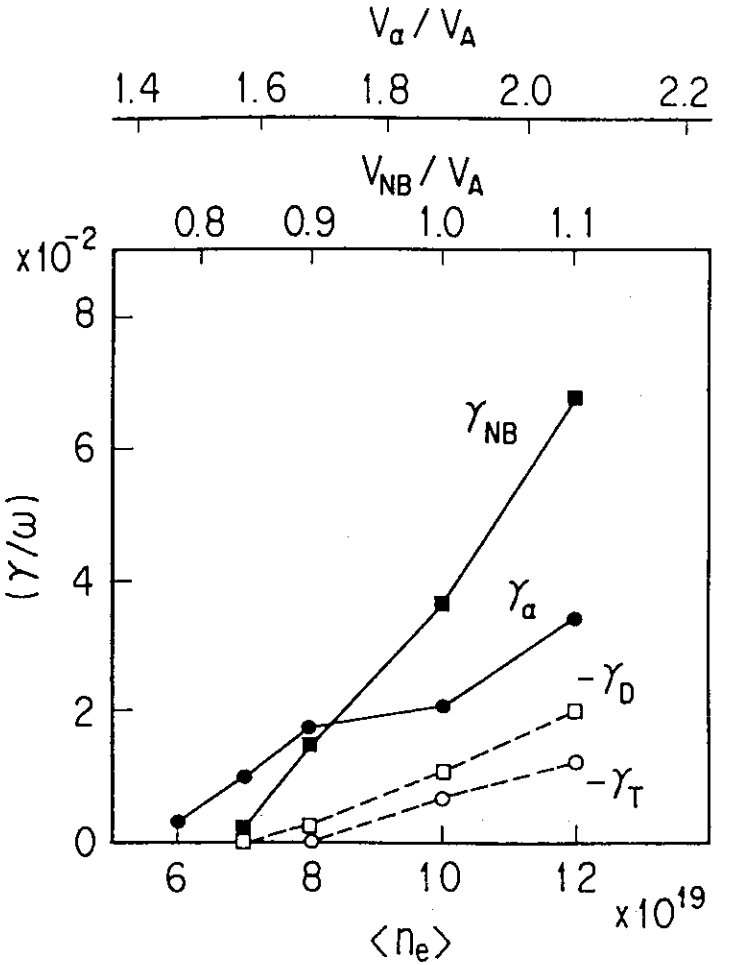

Fig.7 The density $\langle n_e \rangle$ dependence of the grow rates γ_{NB} due to beam particles, the grow rates γ_α due to α particles, the damping rates γ_D due to the Deuterium ion Landau damping and the damping rates γ_T due to the Tritium ion Landau damping for an equilibrium wiht 6MA plasma current, 5.77T toroidal field and T_{io}= 12-18keV.

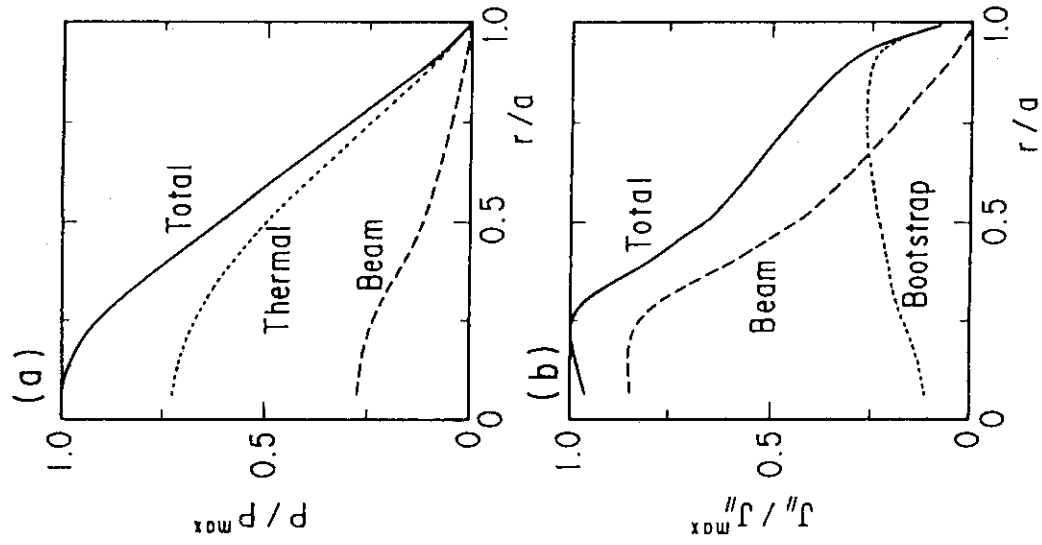

Fig.9 (a) The flux surfaces, (b) the pressure profile and (c) the current profile of the JT-60SU equilibrium, which has 3MA plasma current, 3T toroidal field, $n_{e0} = 7 \times 10^{19}m^{-3}$ and $T_{i0} = 6keV$.

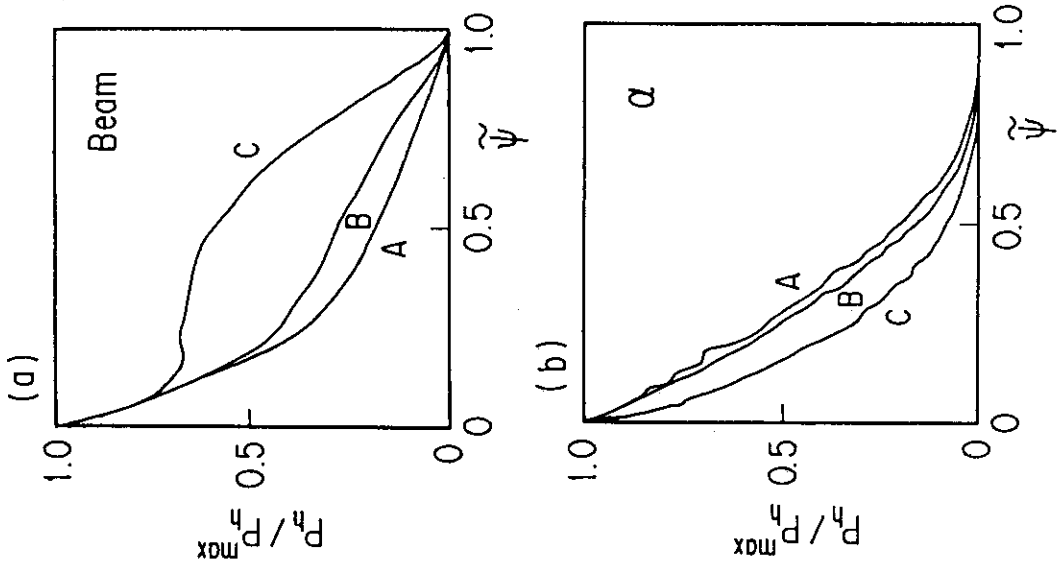

Fig.8 (a) The beam pressure profile and (b) the α pressure profile of A: $\langle n_e \rangle = 6\times10^{19}m^{-3}$ (T_{i0} = 17.7keV), B: $\langle n_e \rangle = 8\times10^{19}m^{-3}$ (T_{i0} = 16.1keV) and C: $\langle n_e \rangle = 12\times10^{19}m^{-3}$ (T_{i0} = 12.7keV) for the equilibria described in Fig.7.

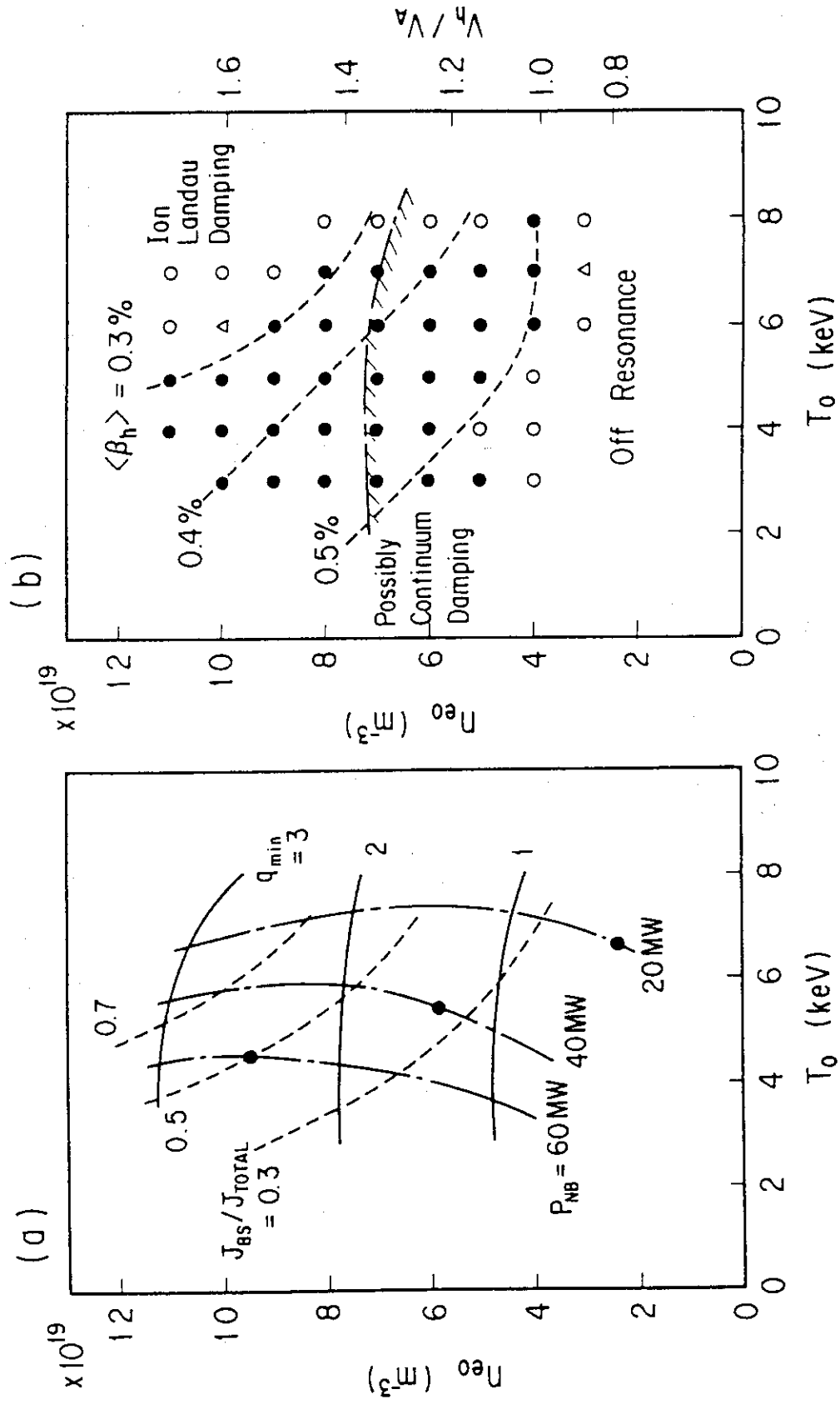

Fig.10 (a) The minimum q-value (solid line), the bootstrap current fraction (broken line) and the required NBI power (dash dotted line) of the equilibrium in the n_{eo} - T_{io} plane.
(b) The stable TAE points (open circle), the unstable (solid circle) points and the marginally stable (triangle) points. The broken curves represent the contours of the beam beta $\langle\beta_h\rangle$.
For $n_{eo} \leq 7\times10^{19}m^{-3}$, the TAE mode crosses the Alfvén continuum.

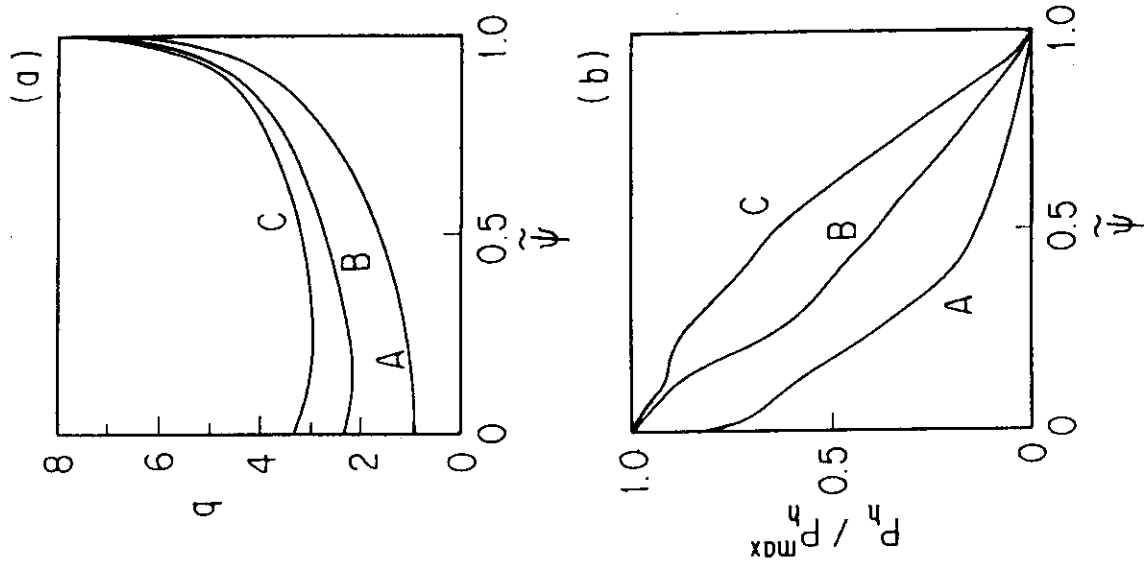

Fig.11 (a) The q-profiles of case A: $n_{e0} = 4 \times 10^{19}m^{-3}$, case B: $n_{e0} = 8 \times 10^{19}m^{-3}$ and case C: $n_{e0} = 11 \times 10^{19}m^{-3}$ of the equilibria with the 3MA plasma current, the 3T toroidal field, and T_{i0} of 5keV.
(b) The corresponding beam pressure profiles P_h.

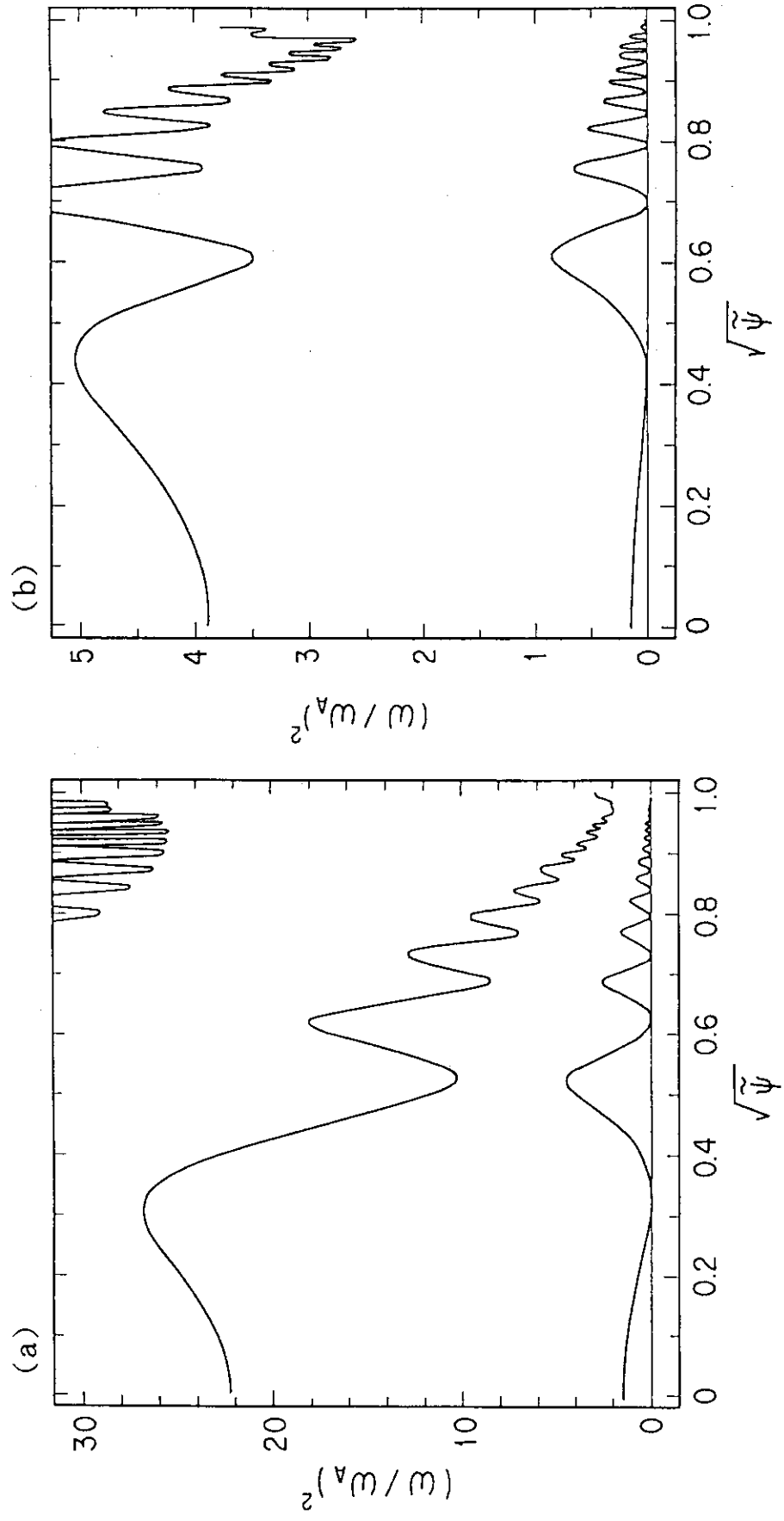

Fig.12 The continuum spectrum for n=3 as a function of the minor radius for the equilibrium of (a) case A, (b) case B, and (c) case C described in Fig.11.

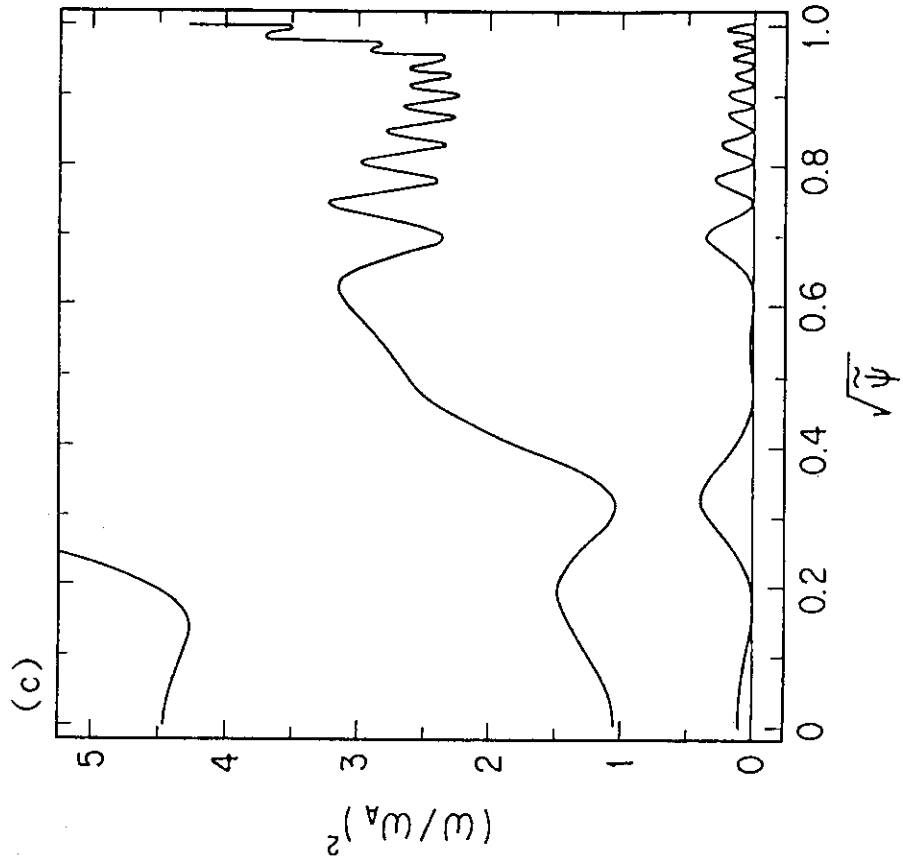

Fig.12 The continuum spectrum for n=3 as a function of the minor radius for the equilibrium of (a) case A, (b) case B, and (c) case C described in Fig.11.

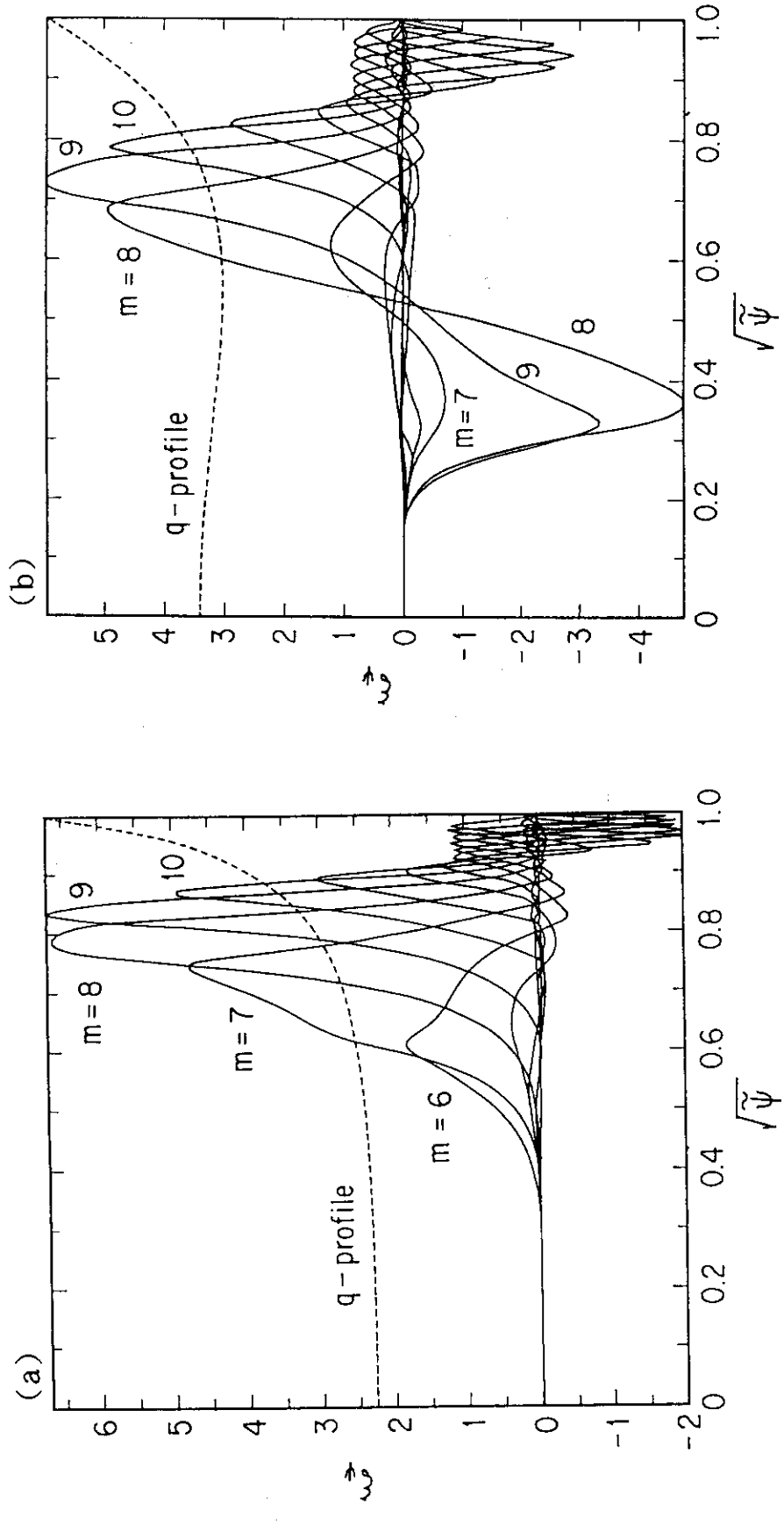

Fig.13 The poloidal harmonics of eigenfunction ξ_ϕ versus the minor radius of (a) the n=3 TAE mode with $(\omega/\omega_A)^2$ of 1.08 for the equilibrium of B in Fig.12, (b) the n=3 TAE mode with $(\omega/\omega_A)^2$ of 0.617 for the equilibrium of C in Fig.12, and (c) the n=3 TAE mode with $(\omega/\omega_A)^2$ of 0.778 for the equilibrium of C in Fig.12.

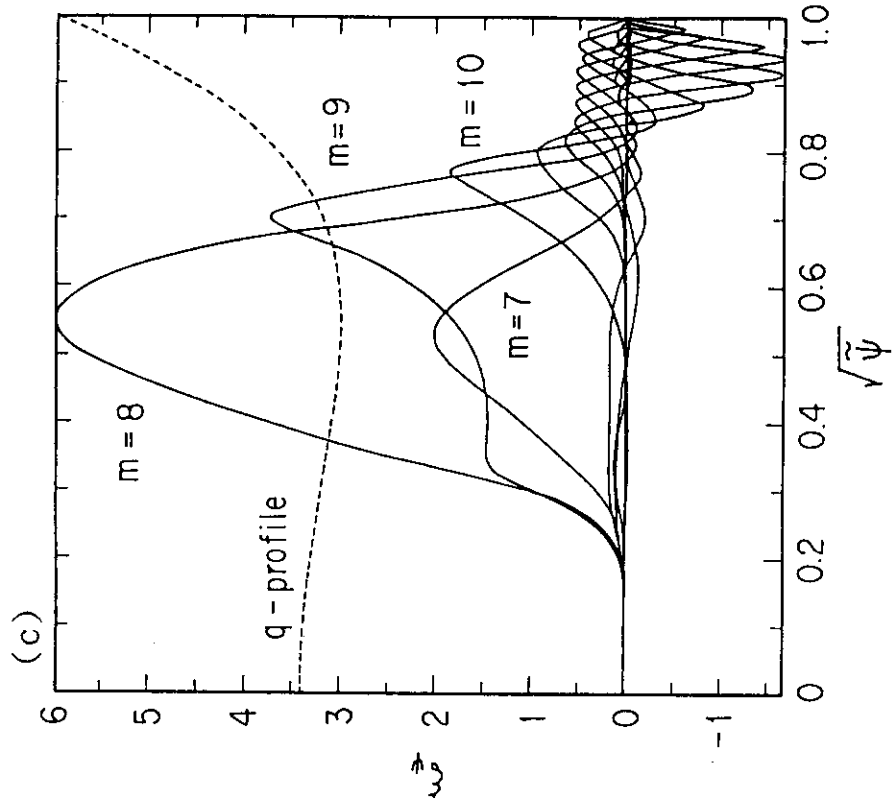

Fig.13 The poloidal harmonics of eigenfunction ξ_ψ versus the minor radius of (a) the n=3 TAE mode with $(\omega/\omega_A)^2$ of 1.08 for the equilibrium of B in Fig.12, (b) the n=3 TAE mode with $(\omega/\omega_A)^2$ of 0.617 for the equilibrium of C in Fig.12, and (c) the n=3 TAE mode with $(\omega/\omega_A)^2$ of 0.778 for the equilibrium of C in Fig.12.